Bioorganic & Medicinal Chemistry Letters xxx (2016) xxx–xxx

Contents lists available at ScienceDirect

Bioorganic & Medicinal Chemistry Letters

journal homepage: www.elsevier.com/locate/bmcl

Identification of potent, selective KDM5 inhibitors

Victor S. Gehling [a,*], Steven F. Bellon [a], Jean-Christophe Harmange [a], Yves LeBlanc [a], Florence Poy [a], Shobu Odate [a], Shane Buker [a], Fei Lan [a], Shilpi Arora [a], Kaylyn E. Williamson [a], Peter Sandy [a], Richard T. Cummings [a], Christopher M. Bailey [a], Louise Bergeron [a], Weifeng Mao [c], Amy Gustafson [b], Yichin Liu [b], Erica VanderPorten [b], James E. Audia [a], Patrick Trojer [a], Brian K. Albrecht [a]

[a] Constellation Pharmaceuticals, Inc., 215 First Street, Suite 200, Cambridge, MA 02142, United States
[b] Genentech, Inc., 1 DNA Way, South San Francisco, CA 94080, United States
[c] WuXi Apptec, 288 Fute Zhong Road, Waigaoqiao Free Trade Zone, Shanghai 200131, China

ARTICLE INFO

Article history:
Received 14 May 2016
Revised 8 July 2016
Accepted 9 July 2016
Available online xxxx

Keywords:
Histone lysine demethylase
KDM5
JARID1
Epigenetics

ABSTRACT

This communication describes the identification and optimization of a series of pan-KDM5 inhibitors derived from compound **1**, a hit initially identified against KDM4C. Compound **1** was optimized to afford compound **20**, a 10 nM inhibitor of KDM5A. Compound **20** is highly selective for the KDM5 enzymes versus other histone lysine demethylases and demonstrates activity in a cellular assay measuring the increase in global histone 3 lysine 4 tri-methylation (H3K4me3). In addition compound **20** has good ADME properties, excellent mouse PK, and is a suitable starting point for further optimization.

Histone methylation plays an important role in the maintenance of chromatin structure and the regulation of transcription.[1] Aberrant changes in histone methylation profiles contribute to cancer development and progression.[2,3] Dynamic regulation of histone lysine methylation states is maintained by the interplay of two enzyme families, histone lysine methyltransferases (KMTs) and demethylases (KDMs).[4] KMTs and KDMs are highly selective for a given histone lysine residue and the number of methyl groups that are added or removed by a given enzyme. The KDM5 (JARID1) proteins (KDM5A, KDM5B, KDM5C, KDM5D) demethylate tri-methylated lysine 4 on histone 3 (H3K4me3), a modification associated specifically with promoters of actively transcribing and transcriptionally poised genes.[5,6] Tumor-promoting and tumor-suppressive roles for the KDM5 family members have been described.[7,8] KDM5A (JARID1A, RBP2) and KDM5B (JARID1B, PLU-1) show increased gene expression in a number of human cancers,[9–14] suggesting that these enzymes may be required for cancer cell survival.

Interestingly, cancer cell subpopulations require KDM5A to acquire reversible tolerance to agents targeting EGF signaling and to cytotoxic agents such as cisplatin.[15] Similarly, KDM5B is implicated in melanoma tumor maintenance and metastatic progression by sustaining a slow cycling subpopulation of cells that is required for the proliferation of the main cancer cell population.[16] In the presence of various anti-cancer agents, including BRAF inhibitors and cisplatin, this KDM5B-expressing melanoma subpopulation gives rise to drug-resistant melanoma cells.[17] Collectively, multiple KDM5 members are implicated in tumor initiation, maintenance, drug tolerance, and suggest that KDM5 inhibitors may have utility as cancer therapeutics.[3,7]

Several KDM inhibitors have been reported towards a variety of targets and this area has recently been reviewed.[18] Many of the literature inhibitors are analogs of the 2-oxoglutarate co-factor (2-OG), such as *N*-oxalyl glycine (NOG), 2,4-pyridine dicarboxylic acid (2,4-PDA), or contain strong metal chelators, such as 2,2-bipyridines or hydroxyquinolines. While these compounds can be potent biochemical inhibitors, in general the literature compounds lack the selectivity profiles necessary to be useful tool compounds and have chemical properties that limit cell permeability. Two reports from GSK have described inhibitors with improved properties and cell-permeability, but these compounds still have significant activity against related KDM's.[19,20] The combination of poor selectivity profiles and limited cell permeability complicates further target validation and drug discovery efforts with the reported KDM5 inhibitors. At the onset of this program our goal was to identify a potent, selective KDM5 inhibitor that could serve as a useful tool to interrogate the contribution of the catalytic activity of KDM5 enzymes in disease biology.

* Corresponding author. Tel.: +1 617 714 0540; fax: +1 617 577 0472.
E-mail address: victor.gehling@constellationpharma.com (V.S. Gehling).

http://dx.doi.org/10.1016/j.bmcl.2016.07.026
0960-894X/

Our initial chemical matter originated from a high throughput screen against KDM4C.[21] Hits from the KDM4C screen were tested against a panel of KDMs representative of the various KDM subfamilies and several compounds were found to inhibit KDM5A with sub-micromolar potency. This effort identified compound **1** as a potent inhibitor of KDM5A with approximately 10-fold selectivity against KDM4C (Fig. 1). Compound **1** serves as an attractive starting point for further optimization as it does not contain an obvious metal chelator or the carboxylic acid functional group common to literature KDM inhibitors.

Attempts to obtain a crystal structure of **1** bound to KDM5A were initially unsuccessful. Due to the difficulty of obtaining co-crystal structures in KDM5A, we used KDM4C as a surrogate for KDM5A. A co-crystal structure of compound **1** bound to KDM4C was solved and this structure was used to determine the mode of inhibition, identify important key interactions, and guide further compound design (Fig. 1).

The crystal structure of **1** bound to KDM4C shows the inhibitor binding in the 2-OG binding site.[22] Compound **1** chelates the catalytic iron via the nitrile functional group while the pyrazolopyrimidine core participates in a well-ordered hydrogen bonding network from lysine 208 and asparagine 282 to both the pyrazole ring and the carbonyl of the inhibitor. One interesting feature of this structure is the movement of tyrosine 134, as this residue swings out of the way to accommodate inhibitor binding.

Using the crystal structure as a rough guide we began assembling our structure activity relationships (SAR) by modifying the 2-methyl group on the pyrazole ring. We replaced the 2-methyl group with an amino-group to afford **2** in an attempt to pick up a favorable interaction with tryptophan 210. This modification was not productive and resulted in a 5-fold loss in potency suggesting that this area of the binding pocket is sensitive to perturbations in the inhibitor structure. Next, we removed the 2-methyl group of **1** to afford **3**. This change resulted in a 12-fold increase in potency relative to **1**. We attribute the increased potency of **3** to removal of unfavorable steric interactions with tryptophan 210 which defines one edge of the binding pocket.

Since the co-crystal structure of **1** bound to KDM4C showed movement of tyrosine 134 we investigated modifications of R^2 in an effort to optimize this interaction. Removal of the ethyl group afforded **4**, a compound that was 15-fold less potent than **1** (Table 1). The reduced potency of compound **4** suggests that the induced fit of compound **1** with tyr134 contributes significantly to the potency of these compounds. In an effort to keep the positive interaction with tyr134 we then examined conservative modifications of the ethyl group, replacing it with an *i*Pr group, as in **5**, and an *n*Pr group, as in **6**. While these modifications were tolerated, they did not afford any improvements in potency over **1**. Extending

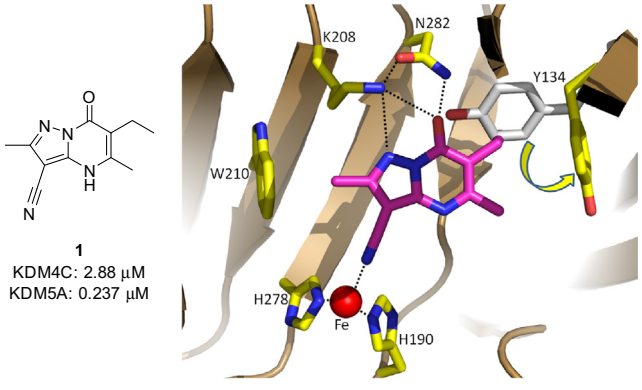

Figure 1. Initial KDM5A hit (**1**) bound to KDM4C.

Table 1
Initial SAR around **1**

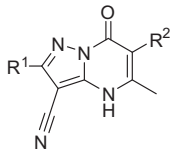

Compound	R^1	R^2	KDM5A IC_{50}[a] (μM)	Standard deviation	LipE[23]
1	Me	Et	0.237[b]	0.065	6.0
2	NH_2	Et	1.18[b]	0.351	6.3
3	H	Et	0.020	0.009	7.5
4	H	H	0.649	0.405	7.0
5	H	*i*Pr	0.024	0.033	7.0
6	H	*n*Pr	0.055[b]	0.013	6.6
7	H	*i*Bu	2.24[b]	0.111	4.5

[a] IC_{50} value reported as an average of ⩾3 determinations with standard deviation reported (SD).
[b] IC_{50} values reported as an average of 2 determinations with standard deviation reported.

the R^2 group to an isobutyl afforded **7**, but this modification led to a significant potency loss. The SAR demonstrates that KDM5 has a well-defined binding pocket formed by tryptophan 210 and tyrosine 134 and that these residues limit the size of substituents at R^2 to small alkyl groups.

After defining the size of the binding pocket, we next investigated changes to the core of the inhibitor (Table 2). We began by cyclizing the R^2 and R^3 groups as in **8**. This modification was not well tolerated, resulting in a compound with weak inhibitory activity against KDM5A. The weak activity of this cyclized compound demonstrates the importance of interacting with tyrosine 134 for potent KDM5A inhibition. We then replaced the pyrazole ring of **8** with an imidazole to afford **9**. This change resulted in a nearly inactive compound against KDM5A and emphasizes the importance of the hydrogen bonding network between inhibitor and protein in affording good KDM5A inhibition (Fig. 1).

Alkylation of the 4-nitrogen was then investigated as these modifications extend into the large substrate binding pocket and would allow us to probe for additional interactions. Alkylation with a methyl group to form **10** resulted in a 10-fold loss in potency. Further potency losses occurred when the alkyl group was extended, as in compound **11**. From the *N*-alkyl analogs, we moved to triazine **12** and methyl ether **13**. Surprisingly, compound **12** was completely inactive against KDM5A, despite the triazine compound containing all of the key recognition elements for binding.

One potential explanation for the absence of activity observed with triazene **12** is that binding to KDM5A requires an acidic hydrogen atom. Whether this acidic hydrogen atom is directly involved with binding to KDM5A or affords access to an active tautomer of the inhibitor is not obvious. What is consistent, from triazene **12** and *N*-alkyl analogs **10** and **11**, is that the absence of an acidic hydrogen atoms is detrimental to KDM5 inhibition.

Exploring our core SAR further, we synthesized methyl ether **13**. Consistent with earlier discussion of the importance of an acidic hydrogen atom, this modification resulted in a ~16 fold loss in activity compared to **3**. As none of our core modifications afforded an advantage relative to the starting point, we focused our attention on the optimization of the right hand side of our inhibitors.

A variety of functional groups were investigated at R^3, including aryl groups, heterocycles, and amides (Table 3). In general aromatic and heteroaromatic groups were well tolerated at R^3 leading to potent KDM5A inhibitors. The only exceptions are the 4-pyridine (**18**) and the *m*-tolyl (**16**) compounds, both of which demonstrate

Table 2
Pyrazolo-pyrimidine core modifications

Compound	Structure	KDM5A IC_{50}[a] (μM)	Standard deviation	LipE
8	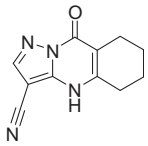	0.878	0.397	5.8
9	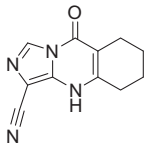	22.5	1.78	3.9
10	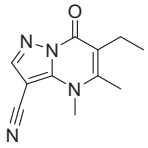	0.214	0.098	6.5
11	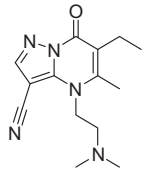	3.09	0.447	5.2
12	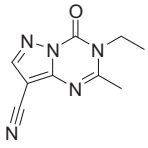	>25	–	–
13	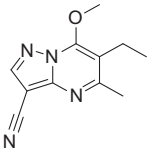	0.324	0.342	4.7

[a] IC_{50} values reported as an average of ⩾3 determinations with standard deviation reported (SD).

Table 3
Optimization of the pyrazolopyrimidine core

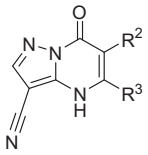

Compound	R^2	R^3	KDM5A IC_{50} (μM)[a]	Standard deviation	LipE
3	Et	Me	0.020[b]	0.009	7.5
14	Et		0.712[b]	0.359	7.0
15	Et		0.015	0.011	6.3
16	Et		0.206	0.144	5.0
17	Et		0.013[b]	0.006	7.9
18	Et		8.94[b]	2.27	5.0
19	Et	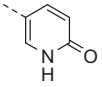	0.011[b]	0.002	9.1
20	*i*Pr		0.010	0.001	6.0

[a] IC_{50} values reported as an average of ⩾3 determinations with standard deviation reported (SD).

[b] IC_{50} values reported as an average of 2 determinations with standard deviated reported.

poor activity against KDM5A. The ethyl amide compound (**14**) was also not well tolerated resulting in significant potency losses. In contrast to the amide and 4-pyridine examples, the 4-pyridone compound (**19**) was among the most potent compounds synthesized with a KDM5A IC_{50} of 11 nM. Finally, combining an isopropyl substituent at R^2 with a phenyl ring at R^3 afforded **20**, a highly potent KDM5A inhibitor with a biochemical IC_{50} of 10 nM.

Compound **20** was profiled in our selectivity panel of KDMs and while it demonstrated nearly equivalent inhibition of the different members of KDM5 family, it displays a remarkable selectivity profile against the other KDMs tested. In particular, **20** is greater than 200 fold selective over KDM4C and has >500 fold selectivity against the other KDMs (Fig. 3). As compound **20** is a potent and selective inhibitor of the KDM5 enzymes, it was profiled in our cellular assays alongside compound **16** which served as an inactive control.

Our KDM5A cellular assay measures the increase of global H3K4me3 levels in PC9 cells upon compound treatment. In this assay compound **20** demonstrated a significant effect on the global level of H3K4me3 with a cellular EC_{50} of 5.2 μM.[21] In the same assay inactive control **16** had no effect on the H3K4me3 mark suggesting that the mark change is due to selective inhibition of the KDM5 family. In an alternative cellular assay with U2OS cells, compound **20** demonstrates a modest increase in H3K4me3 (Fig. 2a, 1.6 fold increase at 30 μM), while inactive control **16** shows no effect. Interestingly, there was a dose-dependent increase in the KDM5B and KDM5C protein levels upon treatment with active compound **20** that was not observed with inactive control **16**. The increased protein levels are not explained by increases in the transcription levels of these proteins and suggests that inhibitor binding stabilizes KDM5B and KDM5C (Fig. 2b).

The poor translation of compound **20** into the cellular assay may be attributed to a variety of causes, including poor permeability, high-intracellular 2-OG concentrations, and/or poor physical properties. In an effort to understand the poor translation of compound **20** into our cellular assay we measured it's permeability in MDCK cells and compound **20** demonstrates good permeability (Papp (A to B) = 17.2×10^{-6} cm/s, Papp (B to A) = 12.1×10^{-6} cm/s) with little efflux observed.[25] Next we generated KDM5A IC_{50} data on compound **20** at two 2-OG concentrations; one at approximately the Km of 2-OG[26] and another with 2-OG concentrations 10-fold above Km (Fig. 3). In these experiments compound **20** displays a modestly shifted IC_{50} of 20 nM in the high 2-OG conditions. Intracellular 2-OG concentrations are reported to be in the high μM range[24] but do not fully explain the >500 fold shift between biochemical and cellular activity observed with compound **20**. Further efforts directed at improving physical properties of the series may afford inhibitors with improved biochemical to cell translation. As compound **20** is a potent, selective, and cell-permeable KDM5 inhibitor it was advanced into our ADME panel and profiled in a mouse PK experiment (Fig. 3).

The synthesis of compound **20** entails a straightforward two step sequence (Fig. 4). The first step is a Claisen condensation of esters **21** and **22** to afford beta-keto ester **23**. Condensation of **23** with the amino-pyrazole **24**[27] affords compound **20** in two steps.

Compound **20** demonstrates low microsomal metabolism and is highly protein bound across species. This profile translates very

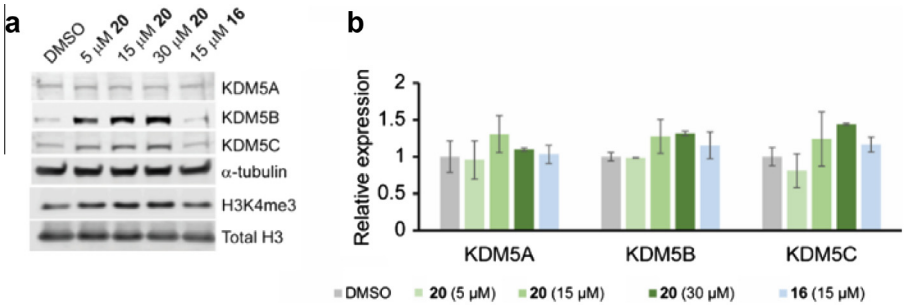

Figure 2. (a) Western blot demonstrating the effect of compound on H3K4me3 levels and KDM5protein levels in U2OS cells. (b) Transcript levels of the KDM5 family proteins upon compound treatment in U2OS cells.

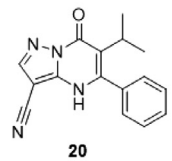

20

KDM5A IC_{50} (μM) = 0.010 ± 0.001 (n = 10)
PC9 H3K4me3 EC_{50} (μM) = 5.2 ± 1.2 (n = 5)

ADME

Species	*Liver microsomes (Clint; mL/min/kg)*	*Plasma protein binding (% bound)*
Mouse	24	98.8
Rat	7.0	99.7
Human	6.0	>99.9

Mouse PK

Parameter	*1 mpk IV*	*5 mpk PO*
$t_{1/2}$ (h)	1.18	3.4
Vss (L/kg)	0.238	-
Cl (mL/min/kg)	4.4	-
AUC (0-last; μM/h)	13.3	62.8
F (%)	-	>100

KDM selectivity (μM)

KDM5A (1 μM 2-OG)	KDM5A (20 μM 2-OG)	KDM5B	KDM5C	KDM2B	KDM3B	KDM4C	KDM6A	KDM7B
0.010	0.020	0.003	0.014	>25, 9.1	>25, 15.3	2.0	>25	7.7

Figure 3. In vitro and in vivo profile of **20**.[21]

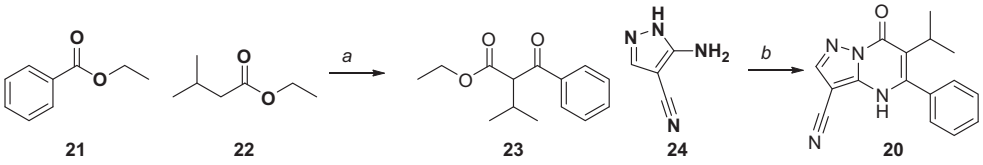

Figure 4. Synthesis of **20**. Reagents: (a) NaH, DME (51%); (b) microwave, 160 °C (2%).

well into mouse PK experiments where **20** demonstrates low clearance, good half-life, low volume, excellent exposure, and high bioavailability.

In this Letter we describe the identification of a KDM4C hit and optimization against KDM5A. This resulted in the identification of **20**, a compound with low nanomolar biochemical potency and micromolar cellular potency in an assay monitoring changes of global H3K4me3 levels. Compound **20** has good ADME properties, excellent mouse PK, and is highly selective for the KDM5 family.[28] Given the unprecedented degree of selectivity compound **20** serves as a useful tool to study the role of KDM5 enzymes in various cellular contexts. The promising ADME and PK properties suggest that compound **20** provides a useful starting point for further optimization and studies directed towards the optimization of this scaffold will be reported in the future.

References and notes

1. Dawson, M. A.; Kouzarides, T. *Cell* **2012**, *150*, 12.
2. Wee, S.; Dhanak, D.; Li, H.; Armstrong, S. A.; Copeland, R. A.; Sims, R.; Baylin, S. B.; Liu, X. S.; Schweizer, L. *Ann. N.Y. Acad. Sci.* **2014**, 30.
3. Højfeldt, J. W.; Agger, K.; Helin, K. *Nat. Rev. Drug Disc.* **2013**, *12*, 917.
4. McGrath, J.; Trojer, P. *Pharmacol. Ther.* **2015**, 1.
5. Christensen, J.; Agger, K.; Cloos, P. A.; Pasini, D.; Rose, S.; Sennels, L.; Rappsilber, J.; Hansen, K. H.; Salcini, A. E.; Helin, K. *Cell* **2007**, *128*, 1063.
6. Benevolenskaya, E. V. *Biochem. Cell Biol.* **2007**, *85*, 435.
7. Rasmussen, P. B.; Staller, P. *Epigenomics* **2014**, *6*, 277.
8. Blair, L. P.; Cao, J.; Zou, M. R.; Sayegh, J.; Yan, Q. *Cancers* **2011**, *3*, 1383.
9. Li, L.; Wang, L.; Song, P.; Geng, X.; Liang, X.; Zhou, M.; Wang, Y.; Chen, C.; Jia, J.; Zeng, J. *Mol. Cancer* **2014**, *13*, 81.
10. Teng, Y.-C.; Lee, C.-F.; Li, Y.-S.; Chen, Y.-R.; Hsiao, P.-W.; Chan, M.-Y.; Lin, F.-M.; Huang, H.-D.; Chen, Y.-T.; Jeng, Y.-M.; Hsu, C.-H.; Yan, Q.; Tsai, M.-D.; Juan, L.-J. *Cancer Res.* **2013**, *73*, 4711.
11. Vieira, F. Q.; Costa-Pinheiro, P.; Ramalho-Carvalho, J.; Pereira, A.; Menezes, F. D.; Antunes, L.; Carneiro, I.; Oliveira, J.; Henrique, R.; Jerónimo, C. *Endocr. Relat. Cancer* **2014**, *21*, 51.
12. Hou, J.; Wu, J.; Dombkowski, A.; Zhang, K.; Holowatyj, A.; Boerner, J. L.; Yang, Z.-Q. *Am. J. Transl. Res.* **2012**, *4*, 247.
13. Xiang, Y.; Zhu, Z.; Han, G.; Ye, X.; Xu, B.; Peng, Z.; Ma, Y.; Yu, Y.; Lin, H.; Chen, A. P.; Chen, C. D. *Proc. Natl. Acad. Sci. U.S.A.* **2007**, *104*, 19226.
14. Hayami, S.; Yoshimatsu, M.; Veerakumarasivam, A.; Unoki, M.; Iwai, Y.; Tsunoda, T.; Field, H. I.; Kelly, J. D.; Neal, D. E.; Yamaue, H.; Ponder, B. A. J.; Nakamura, Y.; Hamamoto, R. *Mol. Cancer* **2010**, *9*, 59.
15. Sharma, S. V.; Lee, D. Y.; Li, B.; Quinlan, M. P.; Takahashi, F.; Maheswaran, S.; McDermott, U.; Azizian, N.; Zou, L.; Fischbach, M. A.; Wong, K.-K.; Brandstetter, K.; Wittner, B.; Ramaswamy, S.; Classon, M.; Settleman, J. A. *Cell* **2010**, *141*, 69.

16. Roesch, A.; Fukunaga-Kalabis, M.; Schmidt, E. C.; Zabierowski, S. E.; Brafford, P. A.; Vultur, A.; Basu, D.; Gimotty, P.; Vogt, T.; Herlyn, M. *Cell* **2010**, *141*, 583.
17. Roesch, A.; Vultur, A.; Bogeski, I.; Wang, H.; Zimmerman, K. M.; Speicher, D.; Korbel, C.; Laschke, M. W.; Gimotty, P. A.; Philipp, S. E.; Krause, E.; Patzold, S.; Villanueva, J.; Krepler, C.; Fukunaga-Kalabis, M.; Hoth, M.; Bastian, B. C.; Vogt, T.; Herlyn, M. *Cancer Cell* **2013**, *23*, 811.
18. McAllister, T. E.; England, K. S.; Hopkinson, R. J.; Brennan, P. E.; Kawamura, A.; Schofield, C. J. *J. Med. Chem.* **2016**, *59*, 1308.
19. Westaway, S. M.; Preston, A. G. S.; Barker, M. D.; Brown, F.; Brown, J. A.; Campbell, M.; Chung, C.; Diallo, H.; Douault, C.; Drewes, G.; Eagle, R.; Gordon, L.; Haslam, C.; Hayhow, T. G.; Humphreys, P. G.; Joberty, G.; Katso, R.; Kruidenier, L.; Leveridge, M.; Liddle, J.; Mosley, J.; Muelbaier, M.; Randle, R.; Rioja, I.; Rueger, A.; Seal, G. A.; Sheppard, R. J.; Singh, O.; Taylor, J.; Thomas, P.; Thomson, D.; Wilson, D. M.; Lee, K.; Prinjha, R. K. *J. Med. Chem.* **2016**, *59*, 1357.
20. Westaway, S. M.; Preston, A. G. S.; Barker, M. D.; Brown, F.; Brown, J. A.; Campbell, M.; Chung, C.; Drewes, G.; Eagle, R.; Garton, N.; Gordon, L.; Haslam, C.; Hayhow, T. G.; Humphreys, P. G.; Joberty, G.; Katso, R.; Kruidenier, L.; Leveridge, M.; Pemberton, M.; Rioja, I.; Seal, G. A.; Shipley, T.; Singh, O.; Suckling, C. J.; Taylor, J.; Thomas, P.; Wilson, D. M.; Lee, K.; Prinjha, R. K. *J. Med. Chem.* **2016**, *59*, 1370.
21. For screening details, biochemical assay descriptions, cell-assay descriptions, and further characterization of compound **20**, see: Vinogradova, M.; Gehling, V. S.; Gustafson, A.; Arora, S.; Tindell, C. A.; Wilson, C.; Williamson, K. E.; Guler, G. D.; Gangurde, P.; Manieri, W.; Busby, J.; Flynn, E. M.; Lan, F.; Kim, H.; Odate, S.; Cochran, A. G.; Liu, Y.; Wongchenko, W.; Yang, Y.; Cheung, T. K.; Maile, T. M.; Lau, T.; Costa, M.; Hegde, G. V.; Jackson, E.; Pitti, R.; Arnott, D.; Bailey, C.; Bellon, S.; Cummings, R. T.; Albrecht, B. K.; Harmange, J. C.; Kiefer, J. R.; Trojer, P. T.; Classon, M. *Nat. Chem. Biol.* **2016**, *12*, 531.
22. The X-ray coordinates for compound **1** bound to KDM4C are available from the PDB, with ID 5KR7.
23. LipE = pIC_{50} – Clog*P*. Clog*P* values were calculated in Chemdraw 15.0.
24. Thirstrup, K.; Christensen, S.; Moller, H. A.; Ritzen, A.; Bergstrom, A. L.; Sager, T. N.; Jensen, H. S. *Pharmacol. Res.* **2011**, *64*, 268.
25. Compound **20** also showed good permeability in MDCK cells expressing MDRI with some efflux observed. MDCK-MDRI Papp (A to B) 8.4×10^{-6} cm/s and Papp (B to A) 27.6×10^{-6} cm/s.
26. 2-OG Km for KDM5A was measured at ~1–2 μM.
27. 3-Aminopyrazole-4-carbonitrile was purchased from Sigma–Aldrich and used without further purification.
28. For further selectivity profiling against a variety of 2-OG utilizing enzymes, see: Joberty, G.; Boesche, M.; Brown, J. A.; Eberhard, D.; Garton, N. S.; Humphreys, P. G.; Mathieson, T.; Muelbauer, M.; Ramsden, N. G.; Reader, V.; Rueger, A.; Sheppard, R. J.; Westaway, S. M.; Bantscheff, M.; Lee, K.; Wilson, D. M.; Prinjha, R. K.; Drewes, G. *ACS Chem. Biol.* **2016**. http://dx.doi.org/10.1021/acschembio.6b00080.